Voltage-controlled three terminal GaAs negative differential resistance device using n^+-i-p^+-i-n^+ structure

K.F. Yarn, MEng
Prof. Y.H. Wang, DEng
Prof. C.Y. Chang, DEng
C.S. Chang, DEng

Indexing terms: Transistors, Semiconductor devices and materials

Abstract: A novel three terminal GaAs n^+-i-p^+-i-n^+ negative differential resistance device prepared by molecular beam epitaxy is demonstrated for the first time. The peak-to-valley current ratios can be modulated by the third external applied voltage which can be expressed as $I_p/I_v = 5.08 \times 10^{-3} \exp [1.999 V_{BE}]$ at room temperature, where V_{BE} is in units of volts. It implies that large peak-to-valley current ratios (e.g. $I_P/I_V = 300$ at $V_{BE} = 5.5$ V) and large peak current densities can easily be obtained just by increasing the V_{BE} bias. A phenomenological bipolar-unipolar transition model is proposed to interpret the observed behavior and confirmed by experiments.

1 Introduction

Recently, the resonant tunnelling of electrons in double barrier semiconductor diodes exhibiting negative differential resistance (NDR) characteristics has drawn many interested parties to pursue the extremely high frequency applications [1–3]. The peak-to-valley current ratios of the improved structures are achieved mainly at low temperature, however, the peak-to-valley current ratios are still low [4]. Double injection structures have also been proposed to obtain the NDR characteristics as functional devices [5, 6]. Kapoor and Henderson have reported a variable N-type negative resistance in an injection diode [5]. Also, Supadech *et al.* reported voltage-controlled negative resistance in p^+-i-n^+ planar diodes with injection gates [6], where there are deep impurity levels are in the i-region. However, for the proposed structures, S-type NDR characteristics are observed at large anode to cathode bias. The peak-to-valley current ratios for the report of Kapoor *et al.* are still low [5]. The valley current is almost half of the peak current. Kastalsky *et al.* reported on an investigation of an NDR transistor with a field effect structure using the difference in GaAs and AlGaAs mobilities [7]. The mechanisms are different from the present work.

Paper 7077G (E3, E10), first received 8th May 1989 and in revised form 6th October 1989

K.F. Yarn and Y.H. Wang are with the Department of Electrical Engineering, National Cheng Kung University, Tainan, Taiwan
C.Y. Chang is with the Institute of Electronics, National Chiao Tung University, Hsinchu, Taiwan
C.S. Chang is with Avantek Inc., Santa Clara, CA 95054, USA

The main purpose of this study is to obtain large and controllable peak-to-valley current ratios using the concept of base channel blocking, i.e. from bipolar to unipolar operation [8]. A simple GaAs homojunction structure is then proposed to realise the concept. Compared to the conventional homojunction transistor, the major difference is the base structure. The base region is formed by a heavily doped thin p^+-layer inserted in two thick undoped layers. A GaAs voltage-controlled N-shape negative differential resistance transistor using the n^+-i-p^+-i-n^+ structure prepared by molecular beam epitaxy (MBE) is demonstrated for the first time. The peak-to-valley current ratios can easily be modulated by the third applied voltage. A large peak-to-valley current ratio and applied bias signal (e.g. $I_p/I_v = 300$ and $P_{max} > 100$ W/cm^2 for $V_{BE} = 5.5$ V at room temperature) can be expected just by increasing the applied base-to-emitter bias. This implies high efficiency and high power operation. The mechanisms are quite different from those previously reported [1–7]. The fabrication process is also easy. In this report, the electrical properties of this novel device are first described. The NDR characteristics are not caused by the heating effect at higher current levels [9, 10]. Hence, a phenomenological bipolar-unipolar transition model is then proposed to interpret the unique device behavior.

2 Experiment

The schematic cross-section of the MBE-grown three terminal GaAs device is illustrated in Fig. 1. Silicon and beryllium were used as n- and p-type dopants, respectively. The growth temperature was kept at 580°C with a growth rate of 1 μm/hr using the arsenic pressure-controlled method [11]. A 0.8 μm thick undoped GaAs layer was first grown on a Si-doped n^+-GaAs substrate, followed by a thin p^+ layer, e.g. 110 Å, with a high doping concentration of 5×10^{18} cm^{-3}. The corresponding sheet concentration is about 5.5×10^{12} cm^{-2}. A 0.4 μm thick undoped GaAs layer was then deposited. Finally, 0.2 μm thick n^+ GaAs layer was grown. A V-groove mesa etching technique was employed to delineate the structure [12]. Au/Ge was deposited and alloyed to facilitate the ohmic contact of the n^+ layers while Au/Zn for the contact of p^+-base. The typical emitter area is about 9×10^{-4} cm^2.

3 Results and discussion

The typical current/voltage characteristics for the NDR device are schematically shown in Fig. 2 for a fixed V_{BE}

bias. The definitions of the specific currents and voltages to be discussed are also illustrated in Fig. 2. N-shape NDR characteristics are revealed clearly. The operation of this device is described as follows. For an applied V_{BE} bias, there is an offset region in $0 \leqslant V_{CE} \leqslant V_{CI}$ (cut-in

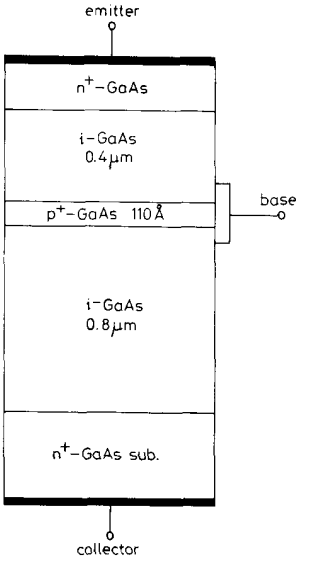

Fig. 1 *Cross-sectional view of the proposed NDR transistor*

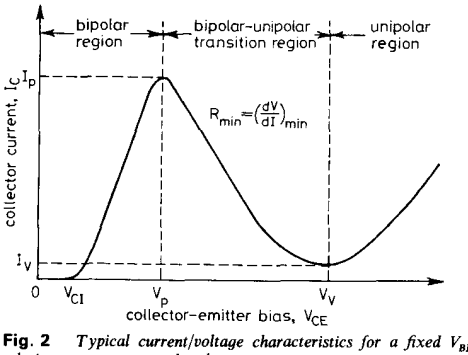

Fig. 2 *Typical current/voltage characteristics for a fixed V_{BE}. The relative parameters are also shown*

voltage). The collector current I_C is suppressed to a very small value for collector-to-emitter voltage V_{CE}, less than V_{CI}, after which I_C increases very rapidly with increasing V_{CE} until V_{CE} reaches V_P, where $I_C = I_P$. This point is followed by N-shape NDR characteristics, i.e. I_C current decreases with increasing V_{CE} bias. As V_{BE} is increased, the peak collector current I_P and collector-to-emitter voltage V_P are also increased. At the voltage of v_v, the collector current is suppressed to a minimum. The corresponding valley voltage V_v increases with increasing V_{BE}. As V_{CE} increases to be larger than V_v, the collector current increases again.

I_C curves as functions of the V_{CE} and V_{BE} are shown in Fig. 3. The V_{BE} bias is 0.5 volts per step. A cut-in voltage is clearly shown in Fig. 3*a*. V_{CI} increases with increasing V_{BE} bias. Fig. 3*b* depicts the N-shape NDR characteristics at various V_{BE} biases. The characteristics of this device operated at 77 K are shown in Fig. 3*c*. It possesses the same characteristics as that at room temperature with increasing V_{CE}. V_P increases with increasing V_{BE}. The negative differential resistance (R_n), $R_n = dV/dI$, decreases with increasing V_{BE} bias. The relation of peak-to-valley current ratios with respect to V_{BE} are shown in Fig. 4.

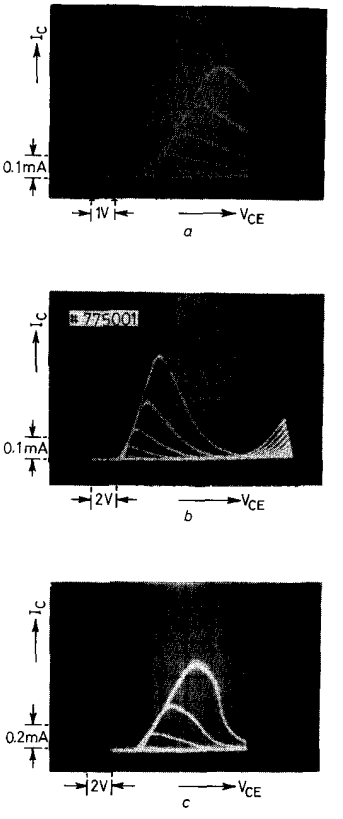

Fig. 3 *I–V characteristics for V_{BE} = 0.5 V/step at (a) 300 K (b) 300 K (c) 77 K*

The inset shown is the *I–V* curves for $V_{BE} = 3.7$ V at 300 K and 77 K, with an emitter area of $\sim 9 \times 10^{-4}$ cm^2. The corresponding peak-to-valley current ratios are 7 and 12, respectively. The peak-to-valley current ratio increases with decreasing temperature. Using the least square method, it can be expressed approximately as

$$I_p/I_v = 5.08 \times 10^{-3} \exp(1.999 V_{BE})$$

for room temperature (1)

and

$$I_p/I_v = 7.32 \times 10^{-3} \exp(1.999 V_{BE}) \quad \text{for 77 K} \qquad (2)$$

where V_{BE} is in units of volts. This suggests that a large peak current density and a large peak-to-valley current ratio can easily be obtained just by increasing the applied V_{BE} bias. For example, the ratio is 40 at $V_{BE} = 4.5$ V, while a ratio of 300 for V_{BE} at 5.5 V is achieved. Also, R_n decreases with increasing V_{BE}, the bias voltage, which may enhance the frequency response. The maximum applied V_{BE} depends on the device geometry and heat sink it can sustain.

The characteristics of the common-base and common-emitter configurations triggered by current are shown in

Fig. 5*a* and 5*b*, respectively. The offset voltage is still observed. The corresponding β ($= I_C/I_B$) and α ($= I_C/I_E$) at $I_B = 0.5$ mA and $I_E = 0.5$ mA are 2 and 0.67, respectively. These low values are reasonable for the high

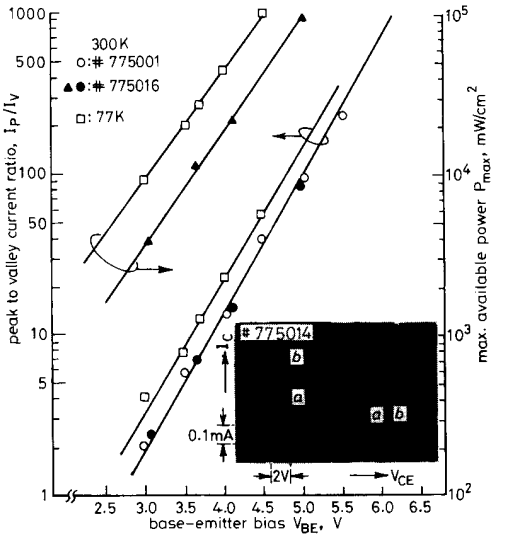

Fig. 4 *The relationship between peak-to-valley current ratios, the calculated maximum available power and V_{BE} at 300 K and 77 K*

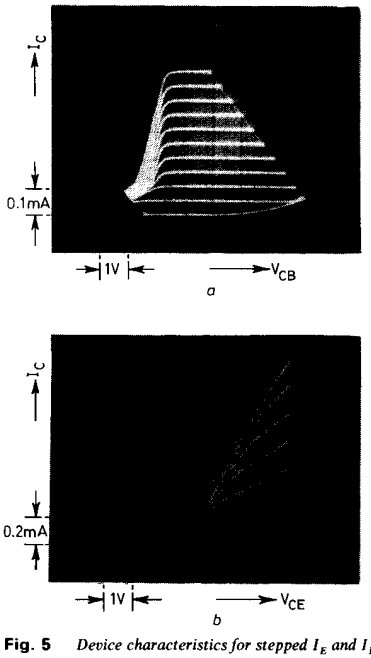

Fig. 5 *Device characteristics for stepped I_E and I_B*
a Common-base characteristics, $I_E = 0.1$ mA/step
b Common-emitter characteristics, $I_B = 0.1$ mA/step

recombination in the heavily doped p^+-base. No NDR characteristics are observed at the same collector current levels. On the other hand, the current gain increases with increasing V_{CE} bias due to the Early effect.

One of the doubtful problems is the observation of the trace in the NDR characteristics. These NDR characteristics are observed frequently in the heterojunction bipolar transistor (HBT) or the FET due to the heating effect, circuit oscillation or charge transfer [9, 10]. The applications of NDR characteristics due to thermal processing are conservative then. Fig. 6 shows the I/V characteristics triggered by an external base bias at V_{BE} =

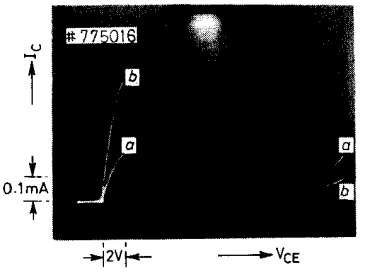

Fig. 6 *I/V characteristics at room temperature*
a $V_{BE} = 3.1$ V
b $V_{BE} = 4.2$ V

3.1 V and 4.2 V for room temperature, respectively. With suitable internal resistance of the curve tracer, no traces are observed in the NDR region of the oscillogram. For the low temperature operation as shown in the inset of Fig. 4, the trace in the NDR region is also not revealed. Referred to Fig. 5 at the same collector current level for the transistor triggered by base current, no NDR characteristics are revealed. The heating effect can be ruled out. Other mechanisms should be developed.

A phenomenological model, a bipolar-unipolar transition model is then proposed to interpret the unique NDR characteristics. The I–V characteristics for a fixed V_{BE} bias are segmented into three regions as shown in Fig. 2 and discussed as follows:

(*a*) Bipolar region for $0 < V_{CE} < V_P$

(*b*) NDR region for $V_P < V_{CE} < V_V$ (Bipolar-unipolar transition region)

(*c*) Unipolar region for $V_V < V_{CE}$.

Fig. 7 sketches the model for the current components and relative parameters. The corresponding neutral base length ($L - L'$), base current and collector current, as a function of V_{CE}, are shown in Fig. 8.

(*a*) *Bipolar region for $0 < V_{CE} < V_P$:* In this region, there is a neutral region in the base and the device can be considered as a conventional bipolar transistor with the collector current increasing with increasing V_{BE} bias, according to the characteristics shown in Fig. 3*a*. V_{CI} increases with increasing V_{BE} bias. This interpretation is due to the leak current of the base. For a small V_{BE} bias, the base current I_B is small. As V_{BE} increases, I_B also increases. At a low constant V_{CE}, for large V_{BE}, I_B increases due to electrons drawn by the forward biased base. The electrons diffused over the base barrier and injected to the collector are reduced. This requires a larger V_{CE} to supply electrons for the same collector current, i.e. V_{CI} increases with increasing V_{BE} bias.

As $V_{CE} > V_{CI}$, the forward bias between base and emitter enhances the electrons injected to the collector, thus, I_C increases with increasing V_{CE}, as with a conventional transistor. As $V_{CE} = V_P$, the collector current reaches a maximum. At this moment, the base width begins to be depleted, i.e. a punch through mode is established. This initialised region is indicated as B' (Fig. 7). As

V_{CE} is further increased above V_P, the effective base channel length ($L - L'$) is decreased while the depletion base length (B'–B' = L') is increased. The corresponding pictures are illustrated in Fig. 8*a*. The current is dominated by diffusion current (J_{diff}) due to a bipolar transistor. For a fixed V_{CE}, I_C increases with increasing V_{BE} as a conventional transistor. I_B is a maximum at $V_{CE} = 0$ for a fixed V_{BE}. I_B decreases with increasing V_{CE} owing to the reduction of recombination in base (Fig. 8*b*).

(b) NDR region for $V_P < V_{CE} < V_V$ (Bipolar-unipolar transition region): The increase in V_{CE} raises the base potential at the point B' shown in Fig. 7. Since the p^+-region is narrow, the spreading resistance is high. The voltage across $R_{BB'}$ is large. The emitter current crowding effect may be serious. The applied V_{CE} is also divided by the resistance of the undoped i-layers, which also plays an important role in the device performance. As the neutral base width at B' for a constant V_{BE} is zero due to the increase in V_{CE}, a forward bias no longer exists between B' and E, i.e. a punch-through mode is established at point B'. $V_{B'E}$ may be driven into reverse bias as compared to V_{BE}. The available neutral base length ($L - L'$) for electrons injected to the collector is decreased resulting in a decreasing of I_C as indicated in Fig. 8, i.e. NDR characteristics occur. The observed results can be confirmed by the fact that V_P increases with increasing V_{BE}. The larger V_{BE}, the larger V_{CE} is required to reach zero base channel width at point B'. V_P as a function of V_{BE} is illustrated in Fig. 9.

As $V_{CE} > V_P$, B' moves toward B with increasing V_{CE}, as illustrated by the arrow shown in Fig. 7. The corresponding neutral base length ($L - L'$) decreases, while depleted base length L' increases as illustrated in Fig. 8*a*. Hence, I_C decreases with increasing V_{CE}. As B' is close to B, i.e. $L - L' = 0$, the base region is fully depleted and can be considered as a planar-doped-barrier device. The current component is then dominated by the thermionic current (J_{th}), while there is no diffusion current. The total current is then the combination of diffusion current and thermionic emission current. The reduction in I_{diff} is larger than the increase in I_{th}. Thus, I_C decreases with increasing V_{CE}.

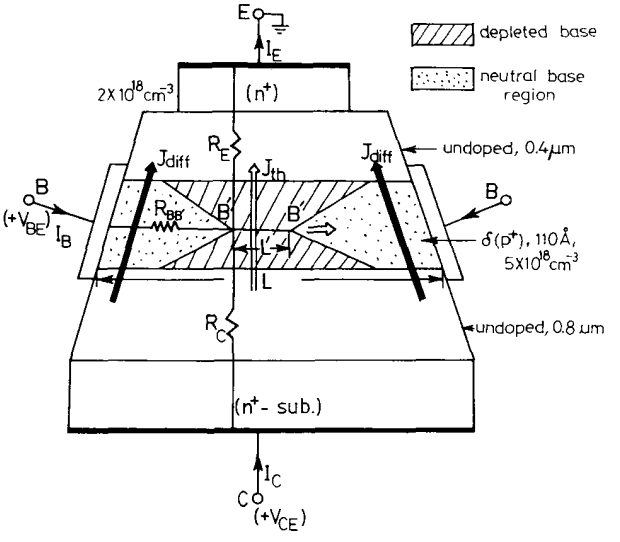

Fig. 7 *Proposed configuration employed to discuss the bipolar-unipolar transition operation*

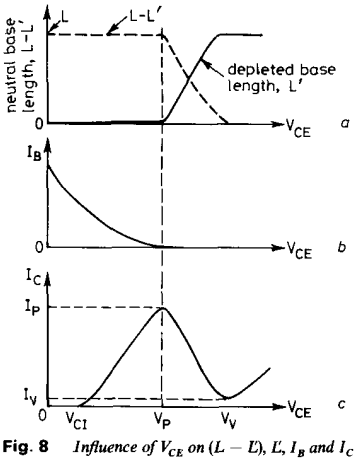

Fig. 8 *Influence of V_{CE} on ($L - L'$), L', I_B and I_C*
a The neutral base length ($L - L'$) and the depleted base length (L') as a function of V_{CE}
b, c The corresponding I_B and I_C

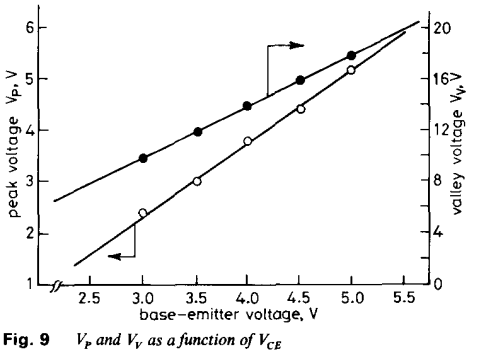

Fig. 9 *V_P and V_V as a function of V_{CE}*

With the increase in p^+-layer thickness to, say, 175 Å, the spreading resistance is reduced. The current-voltage characteristics for this transistor are shown in Fig. 10*a*. The V_{BE} is 0.5 volts per step. The NDR characteristics are not obvious, as are those discussed, for the same trig-

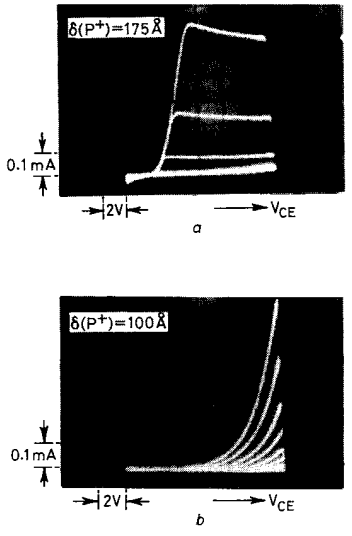

Fig. 10 *The I–V curves for $\delta(p^+)$ = 175 Å and 100 Å.*
V_{BE} = 0.5 V/step

gered levels. The I–V curves for a p^+ layer with a thickness of 100 Å are shown in Fig. 10*b*. They are characteristic of a bulk barrier transistor [12]. An indication of the transition layer thickness of the p^+-layer for the observation of NDR characteristics may be in the range of 100 Å to 175 Å.

(*c*) *Unipolar region for $V_V < V_{CE}$*: In this case, the base is fully depleted at $V_{CE} = V_V$ and can be considered as a planar doped barrier unipolar device [13]. Electrons have more energies to overcome the barrier and be thermionically emitted over it, and so I_C increases again with increasing V_{CE}. The current is dominated by the thermionic emission current. $J = J_{th} + J_{diff} \simeq J_{th}$. An N-shape NDR characteristic is thus formed. The V_V increases with increasing V_{BE} bias as shown in Fig. 9.

The observed NDR phenomenon is attributed to the decrease in the size of the neutral base region. The current components include diffusion current and thermionic current, i.e. the NDR transition occurs due to a combination of bipolar and unipolar devices. In brief, considering the operation of the proposed model, the novel transistor is a bipolar-unipolar NDR (BUNDR) transistor [8].

This can also be confirmed by measuring the base sheet resistance (R_{BB}) and base current (I_B) using the test pattern as shown in Fig. 11. For $V_{CE} = 0$ V, R_{BB} is the smallest value due to the largest neutral base region as shown in Fig. 8 while I_B shows the largest value due to the forward bias of the emitter and the base. When V_{CE} continues to increase, R_{BB}, also increases due to the base channel blocking effect or the decreasing of the base width. As V_{BE} is reduced such that $V_{CE} \geq 16$ V at $V_{BE} =$ 4.5 V, $V_{CE} \geq 14$ V at $V_{BE} = 4$ V and $V_{CE} \geq 12$ V at $V_{BE} =$ 3.5 V, R_{BB} is initially very large and then almost constant, corresponding to the initiation of the unipolar region, V_V. Thus, the estimated valley voltages for $V_{BE} = 4.5$ V, 4 V and 3.5 V are about 16 V, 14 V and 12 V, respectively. They are very consistent with the observation of I–V curves. The trend shown by the measured I_B is also in agreement with the above. When V_{CE} is small, a leakage current is measured from emitter to base. I_B decreases

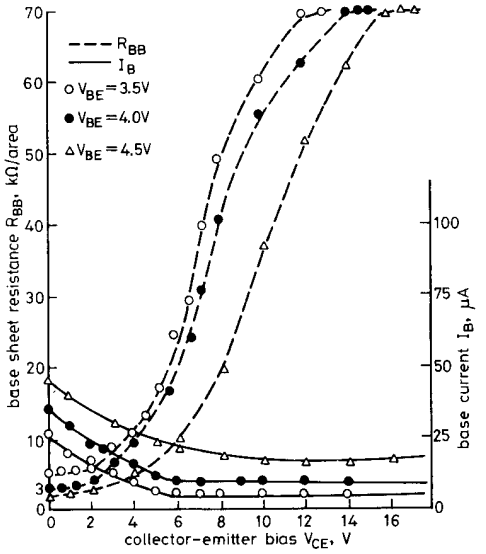

Fig. 11 *Measured sheet resistance R_{BB} and base current I_B as a function of V_{CE}*

with increasing V_{CE} for a fixed V_{BE} due to the decrease in size of the base region. For $V_{CE} \geq V_P$, I_B is reduced to a minimum due to the depleted high resistance base. The measured results support the model proposed. For a change in the polarity of V_{CE}, similar I–V characteristics are also revealed. Furthermore, it is found that the current-voltage characteristics are also geometrical dependent. The cut-in voltage can be reduced to almost zero.*

The maximum available power for such a negative resistance device can be estimated as [14, 15]

$$P_{max} = (3/16)\Delta V \Delta I \tag{3}$$

where $\Delta V(\Delta I)$ is the voltage (current) extent of the negative resistance. A larger power density (e.g. 100 W/cm^2 at $V_{BE} = 5$ V) can also be expected by increasing V_{BE}. The calculated values for 300 K and 77 K are also shown in Fig. 4. High power operation (e.g. $P_{max} > 100$ W/cm^2 at $V_{BE} = 5.5$ V) may be possible.

4 Conclusions

We have reported on a GaAs N-shape negative differential resistance device using the n^+-i-p^+-i-n^+ structure prepared by MBE for the first time. A phenomenological bipolar-unipolar transition model has been proposed to interpret the observed NDR characteristics. It is supported by the measured base sheet resistance and base current. The proposed NDR device possesses the features of

(i) adjustable high peak-to-valley current ratios
(ii) high power operation
(iii) ease of fabrication

* Yarn, K.F., Wang, Y.H., and Chang, C.Y., submitted to be published

The large peak-to-valley current ratios and maximum available power, controlled by the applied base-to-emitter bias, imply the potential for future applications. The microwave potential for such a new NDR device is also developing.

5 Acknowledgments

We are pleased to express our appreciation to those who helped to grow the epilayers and technical assistance, especially M.S. Jame, R.L. Wang and H.R. Sze. Useful discussions were made with Prof. F.Y.T. Kai of Northeastern University. This work is partially supported by the National Science Council of Republic of China under contracts NSC-76-0404-E006-14 and NSC-78-0417-E006-02.

6 References

1 CAPASSO, F., MOHAMMED, H., and CHO, A.Y.: 'Resonant tunneling through double barriers, perpendicular quantum transport phenomena in superlattice, and their device applications', *IEEE Trans.*, 1986, **QE-20**, pp. 1853–1859
2 GOLDMAN, J.G., TSUI, D.C., CUNNINGHAM, J.E., and TSANG, W.T.: 'Transport in double barrier resonant tunneling structures', *J. Appl. Phys.*, 1987, **61**, pp. 2693–2695
3 SEN, S., CAPASSO, F., CHO, A.Y., and SIVCO, D.L.: 'Multiple-state resonant-tunneling bipolar transistor operating at room temperature and its application as a frequency multiplier', *IEEE Electron. Device Lett.*, 1988, **EDL-9**, pp. 533–535
4 HUANG, C.I., PAULUS, M.J., BOZADA, C.A., DUDLEY, S.C., EVANS, K.R., STUTZ, C.E., JONES, R.L., and CHENEY, M.E.: 'AlGaAs/GaAs double barrier diodes with high peak-to-valley current ratio', *Appl. Phys. Lett.*, 1987, **51**, pp. 121–123
5 KAPOOR, A.K., and HENDERSON, H.T.: 'Variable N-type negative resistance in an injection gate double-injection diode', *IEEE Trans.*, 1981, **ED-28**, pp. 275–280
6 SUPADECH, S., OKAZAKI, S., AKIBA, Y., KUROSO, T., and IIDA, M.: 'Voltage-controlled negative resistance in p^+-i-n^+ planar diode with injection gate', *IEE Proc. I, Solid-State Electron Dev.* 1986, **133**, (1), pp. 1–5
7 KASTALSKY, A., BHAT, R., CHAN, W.K., and KOZA, M.: 'Negative-resistance field-effect transistor grown by organometallic chemical vapor deposition', *Solid-State Electron.*, 1986, **29**, pp. 1073–1077
8 YARN, K.F., WANG, Y.H., CHANG, C.Y., and JAME, M.S.: 'A new GaAs bipolar-unipolar transition negative differential resistance device (BUNDR)'. International Electron Device Meeting, Washington D.C., 1987, pp. 74–77
9 HAYES, R., CAPASSO, F., GOSSARD, A.C., MALIK, R.J., and WIEGMANN, W.: 'Bipolar transistor with graded band-gap base', *IEE Electron. Lett.*, 1983, **19**, (11), pp. 410–411.
10 ITO, H., ISHIBASHI, T., and SUGETA, T.: 'High frequency characteristics of AlGaAs/GaAs heterojunction bipolar transistor', *IEEE Electron Device Lett.*, 1984, **EDL-5**, pp. 214–216
11 WANG, Y.H., LIU, W.C., CHANG, C.Y., and LIAO, S.A.: 'Surface morphologies of GaAs layers grown by arsenics-pressure-controlled molecular beam epitaxy', *J. Vac. Sci. Technol.*, 1986, **B4**, (1), pp. 30–36
12 CHANG, C.Y., WANG, Y.H., LIU, W.C., and LIAO, S.A.: 'MBE-grown n^+-i-δp^+-i-n^+ GaAs V-groove barrier transistor', *IEEE Electron Device Lett.*, 1985, **EDL-6**, pp. 123–125
13 MALIK, R.J., AUCOIN, T.R., ROSS, R.L., BOARD, K., WOOD, C.E.C., and EASTMAN, L.F.: 'Planar-doped barriers in GaAs by molecular beam epitaxy', *IEE Electron. Lett.*, 1980, **16**, (22), pp. 836–838
14 SOLLNER, T.C.L.G., TANNENWALD, P.E., PECK, D.D., and GOODHUE, W.D.: 'Quantum well oscillators', *Appl. Phys. Lett.*, 1984, **45**, pp. 1319–1321
15 TRAMBARULO, R.: 'Some X-Band microwave Esaki-diode circuits'. International Solid-State Circuits Conference, Philadelphia, PA, 1961, pp. 18–19